Histone Deacetylase Inhibitors Sensitize Prostate Cancer Cells to Agents that Produce DNA Double-Strand Breaks by Targeting Ku70 Acetylation

Chang-Shi Chen,[1] Yu-Chieh Wang,[1] Hsiao-Ching Yang,[1] Po-Hsien Huang,[1] Samuel K. Kulp,[1] Chih-Cheng Yang,[1] Yen-Shen Lu,[1] Shigemi Matsuyama,[4] Ching-Yu Chen,[2,3] and Ching-Shih Chen[1]

[1]Division of Medicinal Chemistry, College of Pharmacy, The Ohio State University, Columbus, Ohio; [2]Department of Family Medicine, College of Medicine, National Taiwan University; [3]The Gerontology Research Division, The National Health Research Institutes, Taipei, Taiwan; and [4]Department of Pharmacology, Case Western Reserve University, Cleveland, Ohio

Abstract

This study reports a histone deacetylation-independent mechanism whereby histone deacetylase (HDAC) inhibitors sensitize prostate cancer cells to DNA-damaging agents by targeting Ku70 acetylation. Ku70 represents a crucial component of the nonhomologous end joining repair machinery for DNA double-strand breaks (DSB). Our data indicate that pretreatment of prostate cancer cells with HDAC inhibitors (trichostatin A, suberoylanilide hydroxamic acid, MS-275, and OSU-HDAC42) led to increased Ku70 acetylation accompanied by reduced DNA-binding affinity without disrupting the Ku70/Ku80 heterodimer formation. As evidenced by increased Ser^{139}-phosphorylated histone H2AX (γH2AX), impaired Ku70 function diminished cellular capability to repair DNA DSBs induced by bleomycin, doxorubicin, and etoposide, thereby enhancing their cell-killing effect. This sensitizing effect was most prominent when cells were treated with HDAC inhibitors and DNA-damaging agents sequentially. Mimicking acetylation was done by replacing K282, K317, K331, K338, K539, or K542 with glutamine via site-directed mutagenesis, which combined with computer docking analysis was used to analyze the role of these lysine residues in the interactions of Ku70 with DNA broken ends. Mutagenesis of K282, K338, K539, or K542 suppressed the activity of Ku70 to bind DNA, whereas mutagenesis of K317 or K331 with glutamine had no significant effect. Moreover, overexpression of K282Q or K338Q rendered DU-145 cells more susceptible to the effect of DNA-damaging agents on γH2AX formation and cell killing. Overall, the ability of HDAC inhibitors to regulate cellular ability to repair DNA damage by targeting Ku70 acetylation underlies the viability of their combination with DNA-damaging agents as a therapeutic strategy for prostate cancer. [Cancer Res 2007;67(11):5318–27]

Introduction

Histone deacetylase (HDAC) is recognized as one of the promising targets for cancer therapy as aberrant regulation of this epigenetic marking system has been shown to cause the repression of tumor suppressor genes and promotion of tumorigenesis. To date, many HDAC inhibitors have entered human clinical trials in light of their high potency in inhibiting tumor cell growth *in vivo* without incurring significant toxicity (1). Although the effect of HDAC inhibitors on the histone code is well understood, an increasing body of evidence suggests that modulation of gene expression through chromatin remodeling might not be solely responsible for the antiproliferative effects of these agents. This premise is corroborated by the identification of an expanding list of nonhistone proteins as substrates for specific HDACs, including p53, heat shock protein 90, Ku70, androgen receptor, signal transducer and activator of transcription 3, nuclear factor-κB, and α-tubulin (2). Alteration of the acetylation status of these proteins interferes with many signaling processes involved in cell proliferation and survival. More recently, we showed that HDAC inhibitors facilitated Akt dephosphorylation in cancer cells by altering the dynamics of HDAC-protein phosphatase 1 complexes (3). Together, these histone acetylation-dependent and histone acetylation-independent mechanisms underscore the pleiotropic antitumor effects of HDAC inhibitors, at both epigenetic and cellular levels.

In this study, we investigated a histone acetylation-independent mechanism by which HDAC inhibitors sensitize cancer cells to DNA-damaging agents. We hypothesized that HDAC inhibitors mediate this chemosensitization through the modulation of the acetylation status of Ku70, a nonhistone substrate of HDAC. Ku70 forms a heterodimeric Ku protein complex with Ku80, which represents a crucial component of the nonhomologous end joining (NHEJ) DNA double-strand break (DSB) repair machinery (see ref. 4 for review). In cooperation with Ku80, Ku70 binds and bridges two proximal broken DNA ends, which facilitates DNA end-joining through a cascade of reactions that involve DNA-dependent protein kinase and DNA ligase IV. Ku70 contains two DNA-binding domains at NH_2 and COOH termini, both of which are required for the high binding affinity to DNA (5–8). Recent evidence indicates that the COOH terminus of Ku70 also binds Bax and suppresses its apoptotic translocation to mitochondria (9, 10). Consequently, Ku70 mediates its cytoprotective function though two distinct mechanisms (i.e., DNA repair and maintenance of mitochondrial integrity; ref. 11). Increased Ku70 activity would enhance the ability of cells to repair the DNA damage and simultaneously would reduce the tendency to initiate Bax-mediated apoptosis. The dual activity of Ku might be regulated at both transcriptional and post-translational levels in response to apoptotic stimuli. Especially, it is noteworthy that Ku70 is targeted for acetylation and deacetylation by histone acetyltransferases and HDACs, respectively, *in vivo* (12–14). Evidence indicates that increased acetylation levels of Ku70, as a result of HDAC inhibition, abolish its ability of to bind Bax and suppress Bax-mediated apoptosis (12–14). Although acetylation also occurs in the DNA-binding domains of Ku70, the consequent effect on DNA DSB repair remains unclear. Here, we

Requests for reprints: Ching-Shih Chen, Division of Medicinal Chemistry, College of Pharmacy, The Ohio State University, Parks Hall, 500 West 12th Avenue, Columbus, OH 43210. Phone: 614-688-4008; Fax: 614-688-8556; E-mail: chen.844@osu.edu.

doi:10.1158/0008-5472.CAN-06-3996

report that treatment with HDAC inhibitors or mimicking acetylation in the DNA-binding domains of Ku70 diminishes cellular ability to repair drug-induced DNA damage, thereby sensitizing cancer cells to agents producing DNA DSBs.

Materials and Methods

Cell culture. DU-145, LNCaP, and PC-3 prostate cancer cells were purchased from the American Type Culture Collection. These cancer cells were cultured in 10% fetal bovine serum (FBS)–supplemented RPMI 1640 containing 100 units/mL penicillin and 100 μg/mL streptomycin (Life Technologies).

Reagents. The HDAC inhibitors suberoylanilide hydroxamic acid (SAHA), MS-275, and OSU-HDAC42 [a.k.a. (*S*)-HDAC-42] were synthesized in the authors' laboratory. OSU-HDAC42 belongs to a novel class of hydroxamate-tethered phenylbutyrate derivatives with nanomole per liter potency in HDAC inhibition (15–17) and is currently undergoing preclinical testing under the Rapid Access to Intervention Development program at the National Cancer Institute. Trichostatin A (TSA) and bleomycin were purchased from Sigma-Aldrich, and etoposide (VP-16) and doxorubicin were purchased from Calbiochem. Antibodies against various proteins were obtained from the following sources. Mouse monoclonal antibodies: Ku70, Flag, α-tubulin, and acetylated α-tubulin (Sigma-Aldrich); p21 and nucleolin (C23; Santa Cruz Biotechnology); Ser^{139}-phosphorylated histone H2AX (γH2AX) and H2AX (Upstate Biotechnology); and β-actin (ICN Biomedicals). Rabbit polyclonal antibodies: Ku80 and pan-acetylated-lysine (Santa Cruz Biotechnology); Bax (Cell Signaling Technology); and acetyl-histone H3 (Upstate Biotechnology). Agarose-conjugated goat polyclonal anti-Ku70 antibodies were purchased from Santa Cruz Biotechnology, and goat anti-rabbit IgG-horseradish peroxidase (HRP) conjugates and rabbit anti-mouse IgG-HRP conjugates were from Jackson ImmunoResearch Laboratories. Antimouse IgG-Alexa Fluor 488 antibodies were purchased from Molecular Probes. Plasmids encoding various Ku70 mutants were generated by site-directed mutagenesis of pCMV2B Flag-tagged Ku70 (9) by using a QuickChange site-directed mutagenesis kit from Stratagene.

Immunoblotting. Cells treated with various concentrations of HDAC inhibitors in 10% FBS supplemented RPMI 1640 for various time intervals were collected and lysed by NP40 lysis buffer [50 mmol/L Tris-HCl (pH 7.5), 120 mmol/L NaCl, 1% (v/v) NP40, 1 mmol/L EDTA, 50 mmol/L NaF, 40 mmol/L β-glycerophosphate, 1 μg/mL each of aprotinin, pepstatin, and leupeptin]. Protein concentrations of cell lysates were determined by using a Bradford protein assay kit (Bio-Rad). Equivalent amounts of proteins from each lysate were resolved by SDS-PAGE and then transferred onto nitrocellulose membranes (Millipore) in a semidry transfer cell. The transblotted membrane was washed twice with TBS containing 0.1% Tween 20 (TBST). After blocking with TBST containing 5% nonfat milk for 40 min, the membrane was incubated with an appropriate primary antibody in TBST containing 1% nonfat milk at 4°C overnight. All primary antibodies were diluted in 1% nonfat milk-containing TBST. After treatment with the primary antibody, the membrane was washed twice with TBST for a total of 20 min, followed by goat anti-rabbit or anti-mouse IgG-HRP conjugates for 1 h at room temperature, and washed thrice with TBST for a total of 1 h. The immunoblots were visualized by enhanced chemiluminescence (Pharmacia).

Immunoprecipitation of Ku70. The immunoprecipitation was carried out according to a reported procedure (12). In brief, DU-145 cells were treated with various concentrations of HDAC inhibitors for 48 h and lysed by CHAPS lysis buffer [150 mmol/L sodium chloride, 10 mmol/L HEPES (pH 7.4), 1.0% CHAPS] with a cocktail of protease inhibitors (Sigma-Aldrich). After centrifugation at 13,000 × *g* for 15 min, the supernatants were collected and incubated with protein A-Sepharose beads for 15 min to eliminate nonspecific binding. The mixture was centrifuged at 1,000 × *g* for 5 min, and the supernatants were incubated with agarose-conjugated goat polyclonal anti-Ku70 antibodies followed by three washes in 0.1% Triton X-100 in PBS. The immunocomplex was separated by SDS-PAGE and proteins were detected with mouse monoclonal anti-Ku70, Ku80, and rabbit polyclonal anti-pan-acetylated lysine (pan-AcK).

Transfection of Flag-tagged Ku70 expression plasmids. DU-145 cells were nucleofected with individual plasmids encoding Flag-tagged Ku70 and various Ku70 mutants by using a Nucleofactor kit L (Amaxa) as described by the manufacturer. Transfection efficiency was at least 75% in DU-145 cells, as determined by pmaxGFP plasmid transfection (data not shown).

Nuclear protein extraction and DNA end-binding activity of Ku70. Preparation of nuclear extracts and assessment of DNA end-binding activity of Ku70 were carried out by using a Nuclear Extract kit and a Ku70/Ku80 DNA Repair kit, respectively (Active Motif). In brief, Ku70-containing nuclear proteins were extracted from drug-treated or nucleofected cells by a Nuclear Extract kit. Protein concentrations of nuclear extracts were determined by using a Bradford protein assay kit. Further quantification of protein loading amounts was determined by immunoblotting against Ku70 or Flag. Equivalent amounts of proteins (2.5 μg) from each lysate were loaded into a 96-well plate, of which each well contained immobilized linear oligonucleotides with blunt ends. Ku70 protein extracted from the nucleus could specifically bind to this oligonucleotide. The primary antibody used in the Ku70/Ku86 DNA Repair kit recognized an epitope on Ku70 protein that was accessible on DNA binding. Anti-Flag antibody was also used in the experiment for the transfection of Flag-tagged Ku70 plasmids. Addition of a secondary HRP-conjugated antibody provided a sensitive colorimetric readout quantified by spectrophotometry.

Cell survival assay. Survival curves for DU-145 cells were obtained by the clonogenic assay as described previously (18). Cells were plated at 800 to 1,000 cells per plate and exposed to 0.25 μmol/L OSU-HDAC42 for 4 h or DMSO vehicle before exposure to the DSB-inducing drugs. After washing out the HDAC inhibitor, the cells were exposed to increasing amounts of bleomycin (0–100 μg/mL), doxorubicin (0–500 nmol/L), VP-16 (0–50 μmol/L), or 5-fluorouracil (5-FU; 0–1,000 μmol/L) for 1 h. The drugs were then washed away, and the cells were allowed to grow for 14 days. The colonies were fixed and stained with crystal violet (0.5% in 70% ethanol). Colonies containing more than 50 cells were scored. The survival fraction was calculated based on the number of colonies formed in drug-treated cells relative to that of the untreated control. Each dose was done in triplicate, and the experiments were repeated at least twice.

Apoptosis assay. Drug-induced apoptotic cell death was assessed using the Cell Death Detection ELISA kit (Roche Diagnostics), which quantitates cytoplasmic histone-associated DNA fragments in the form of mononucleosomes or oligonucleosomes. Cells were seeded and incubated at 8,000 cells per well in 12-well flat-bottomed plates in 10% FBS-supplemented RPMI 1640. After 24 h, cells were treated with OSU-HDAC42 for 4 h followed by bleomycin, doxorubicin, and VP-16 at the indicated concentrations for 24 h. Both floating and adherent cells were collected and the assay was done according to the manufacturer's instructions.

Immunocytochemical detection of γH2AX foci formation. All experiments were carried out in 10% FBS-supplemented RPMI 1640. Cells were seeded on coverslips at a density of 2×10^5 per slip and incubated overnight. These cells were treated with 0.25 μmol/L OSU-HDAC42 for 4 h, washed, and exposed to DMSO vehicle, 10 μg bleomycin, 100 nmol/L doxorubicin, or 10 μmol/L VP-16 for 1 h. Drug-treated cells were fixed in 100% methanol at −20°C for 30 min, rehydrated in PBS containing 0.1% Triton X-100 for 10 min, and treated with mouse monoclonal anti-γH2AX antibody followed by antimouse IgG-Alexa Fluor 488 antibody. The coverslips were mounted on slides with mounting solution containing 1 μg/mL 4′,6-diamidino-2-phenylindole (DAPI) and observed under an Eclipse TE300 fluorescence microscope (Nikon). Cell nuclei containing at least five condensed fluorescence dots were considered foci positive, and 200 to 300 cells were counted in each slide to estimate the percentage of foci-positive cells in the whole cell population.

Flow cytometric analysis of γH2AX and DNA. Cells (2×10^5) were treated with three DNA-damaging agents as indicated, harvested, and resuspended in PBS containing 40% ethanol for overnight fixation. Following rehydration in PBS and perforation in PBS containing 0.1% Triton X-100, cells were incubated in PBS containing mouse monoclonal antibody against human γH2AX for 30 min at room temperature. After a thorough wash, cells were exposed to antimouse IgG-Alexa Flour 488 antibodies for 30 min at room temperature, washed, and incubated in PBS

containing 1 μg/mL propidium iodide for 20 min at room temperature to label DNA. All samples were analyzed using a fluorescence-activated cell sorter (FACSCalibur, Becton Dickinson Immunocytometry Systems) equipped with CellQuest software.

Molecular modeling analysis of the interaction of Ku70/Ku80 heterodimer with DNA. Protein sequence of human Ku70 (accession no. P23475) was retrieved from the National Center for Biotechnology Information Reference Sequence Collection. Structure of the Ku70/Ku80 complex was constructed by using the Modeller program (19) with the published crystal structures of Ku heterodimer (RCSB entry code, 1JEY and 1JRR) as a modeling template. Subsequently, this Ku heterodimer structure was subject to the addition of polar hydrogens and the assignment of Kollman charges (20). Three-dimensional affinity grids centered on the preformed channel with 0.375-Å spacing were calculated for each of the following atom types: (*a*) Ku protein, A (aromatic C), C, H, N, and O and (*b*) DNA, C, A, N, O, P, H, e (electrostatic), and d (desolvation) using Autogrid3 (21). AutoDock version 3.0.0 was used for the docking simulation. The DNA ligand structure was extracted from the published crystal structure of Ku heterodimer (RCSB Protein Data Bank; PDB ID, 1JEY; ref. 22). We identified six lysine residues in Ku70 that are targets for acetylation in docking simulation, of which K282, K317, K331, and K 338 are located within the ring structure, whereas K539 and K542 lie within the COOH-terminal linker. The broken DNA was docked into the putative Ku preformed channel that exhibits a polarization of positive electrostatic charge focused on the inner surface of the channel and along the DNA-binding cradle (22). The Lamarckian genetic algorithm was used for DNA conformational searching because it has enhanced performance relative to simulated annealing or the simple genetic algorithm. Accordingly, docking simulations of the DNA-Ku binding were carried out by using molecular mechanics with the following variables: trials of 100 dockings, population size of 150, random starting position and conformation, translation step ranges of 2.0 Å, rotation step ranges of 50°, elitism of 1, mutation rate of 0.02, crossover rate of 0.8, local search rate of 0.06, and 100 million energy evaluations. Final docked conformations were clustered using a tolerance of 1.5 Å root mean square deviation.

Statistical analysis. At least three independent experiments were done for all clonogenic assays, apoptosis assay, and immunocytochemical and flow cytometric analyses of γH2AX formation. By using the software package Calcusyn (Biosoft), the values of IC_{50}, the drug concentration required for 50% growth inhibition, were calculated. Statistical differences in DNA-binding affinity and γH2AX formation between drug-treated cells versus controls were determined by two-sided, unpaired Student's *t* test. For statistical analysis, a statistically significant difference was defined as $P < 0.05$.

Results

This study was aimed at investigating the intricate role of Ku70 acetylation in the effect of HDAC inhibitors on sensitizing prostate cancer cells to agents that generated DNA DSBs. In light of the dual function of Ku70 in regulating DNA repair and Bax-mediated apoptosis (9, 10, 14), we chose DU-145 prostate cancer cells as a model based on the following considerations. First, DU-145 cells are deficient in Bax expression (Fig. 1*A*). As the cytoprotective activity of Ku70 works, in part, through inhibition of Bax (9, 10, 14), use of DU-145 cells would allow the assessment of the functional role of Ku70 acetylation in the absence of Bax-mediated apoptosis. Second, DU-145 cells lack functional p53 (23), thereby eliminating the complication of p53 activation in response to apoptotic signals that produce DNA DSBs. Third, expression levels of Ku70 and Ku80 in DU-145 cells were similar to that of PC-3 and LNCaP cells.

Pretreatment with HDAC inhibitors sensitizes prostate cancer cells to agents that generate DNA DSBs. The ability of HDAC inhibitors to enhance the cell-killing effect of drugs known to produce DNA DSBs, including bleomycin, doxorubicin, and VP-16, was shown in Fig. 1*B*. The IC_{50} of OSU-HDAC42 in suppressing DU-145 cell proliferation was 0.4 μmol/L at 72 h (17). DU-145 cells were exposed to 0.25 μmol/L OSU-HDAC42 or DMSO vehicle in 10% FBS-supplemented medium for 4 h, washed with fresh medium, treated with different doses of individual agents for 1 h, and plated for clonogenic cell survival. As shown, a 4-h exposure to OSU-HDAC42 alone over a dose range of 1 nmol/L to 1 μmol/L exhibited no appreciable effect on reducing cell survival (Fig. 1*B, a*). This is in line with our previous report that OSU-HDAC42 and other HDAC inhibitors showed no profound antiproliferative effect in DU-145 cells within 24 h (17). When DU-145 cells were treated with the DNA-damaging agent alone, the IC_{50} values for bleomycin, doxorubicin, and VP-16 were 9.1 μg/mL, 225 nmol/L, and 4.5 μmol/L, respectively (Fig. 1*B, b–d*). In contrast, pretreatment of DU-145 cells with 0.25 μmol/L OSU-HDAC42 for 4 h shifted the dose response curves to the left with the respective IC_{50} values of 1.3 μg/mL, 65 nmol/L, and 0.4 μmol/L, indicating a 3- to 11-fold enhancement in chemosensitivity. This effect, however, was not noted in cells treated with 5-FU (Fig. 1*B, e*), an agent that causes minimum DNA damage (24–26).

The effect of OSU-HDAC42 on chemosensitization was, at least in part, attributable to its ability to augment cellular susceptibility to drug-induced apoptosis. DNA fragmentation ELISA indicates that pretreatment of cells with 0.25 μmol/L OSU-HDAC42 for 4 h significantly increased the extent of nucleosome formation in response to bleomycin, doxorubicin, and VP-16 in a dose-dependent manner ($P < 0.05$ compared with individual drug treatment alone; Fig. 1*C*).

It is noteworthy that this chemosensitizing effect was less prominent when the sequence of drug treatment was revised (i.e., treatment with a DNA-damaging agent preceded OSU-HDAC42 exposure; data not shown). In the literature, a similar finding has also been reported with the combination of TSA and VP-16 (27). We rationalized that pretreatment with the HDAC inhibitor weakened the cellular ability to repair DNA DSBs, rendering cells vulnerable to these DNA-damaging agents. However, this preemptive effect would be less effective once the cells have undergone DNA damage.

Together, these findings suggested the chemosensitizing effect of HDAC inhibitors could be attributed to its ability to suppress DNA DSB repair activity. Among various components of the NHEJ DNA DSB repair pathway (4), Ku70 was especially noteworthy because it is targeted for deacetylation by HDACs.

HDAC inhibition leads to increased acetylation and reduced DNA end-binding affinity of Ku70. Pursuant to the above premise, we characterized the effect of four different HDAC inhibitors, including OSU-HDAC42, SAHA, MS-275, and TSA, on Ku70 acetylation vis-à-vis various HDAC-related biomarkers (histone H3 acetylation, p21 expression, and α-tubulin acetylation) in DU-145 cells. Compared with the other three inhibitors, MS-275 exhibits a narrower spectrum of HDAC isozyme specificity, with inhibitory activity limited to the class I HDACs (HDAC1, HDAC2, and HDAC3; ref. 1). Consequently, although all these agents caused substantial increases in histone H3 acetylation and p21 expression, MS-275 differed from the other three inhibitors in its inability to inhibit the α-tubulin deacetylase HDAC6, a class IIb enzyme (Fig. 2*A*). As shown, OSU-HDAC42, SAHA, and TSA were able to produce robust hyperacetylation of α-tubulin, whereas MS-275 was ineffective in inhibiting α-tubulin deacetylation. Moreover, we examined the effect of these inhibitors on the expression level of Ku70 and Ku80 in light of a recent report that butyrate

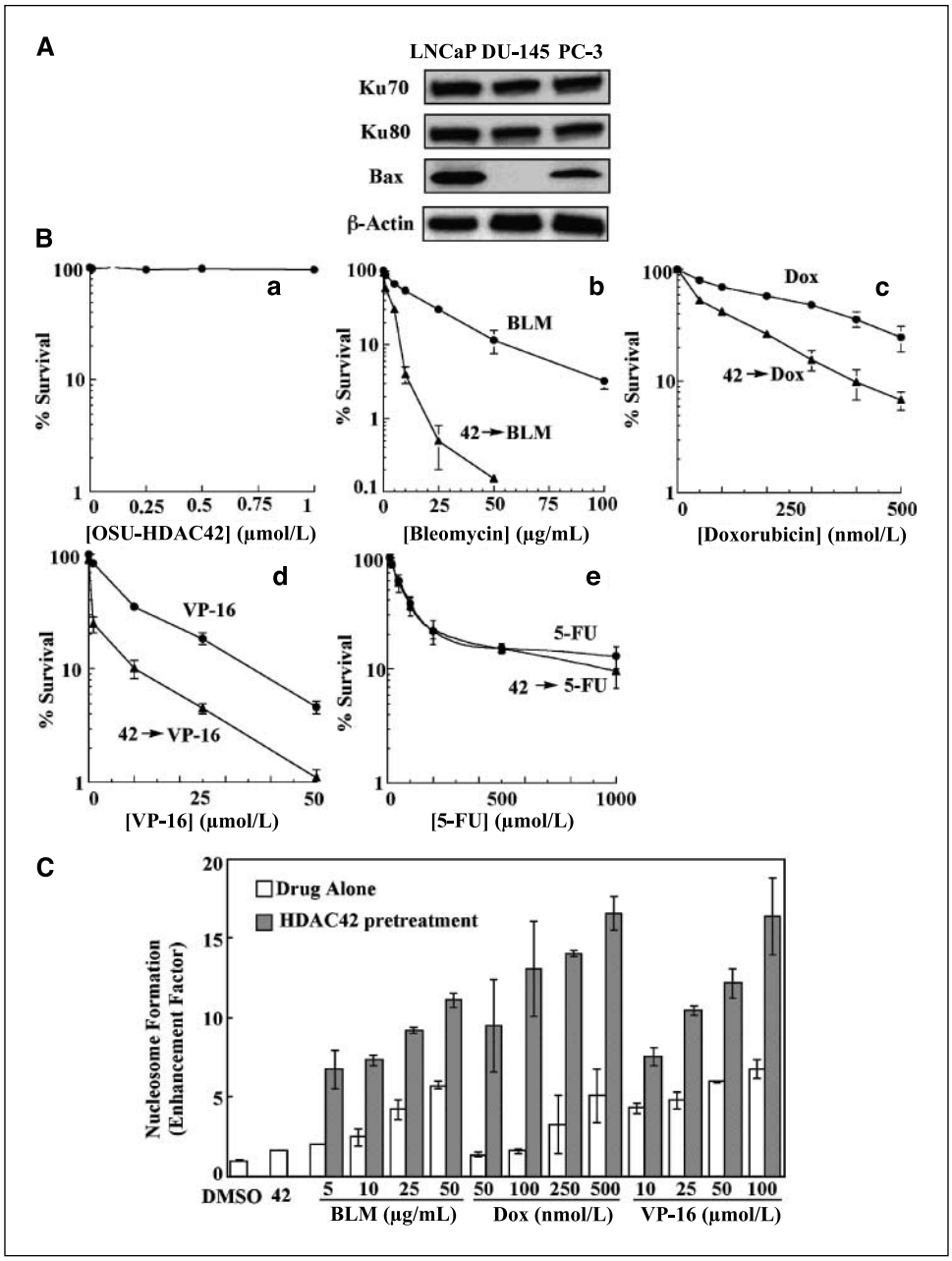

Figure 1. Effect of OSU-HDAC42 on sensitizing DU-145 prostate cancer cells to DNA DSB–inducing agents. *A,* expression levels of Ku70, Ku80, and Bax in three prostate cancer cell lines, LNCaP, DU-145, and PC-3. *B,* pretreatment of DU-145 cells with 0.25 μmol/L OSU-HDAC42 augments the effect of bleomycin (*BLM*), doxorubicin (*Dox*), and VP-16, but not 5-FU, on clonogenic inhibition. Clonogenic survival was analyzed as described in Materials and Methods. *Points,* mean of six replicates. *C,* effect of 0.25 μmol/L OSU-HDAC42 pretreatment on drug-induced DNA fragmentation in DU-145 cells. Cells were treated with 0.25 μmol/L OSU-HDAC42 or DMSO vehicle for 4 h followed by individual agents at the indicated concentrations for 24 h. Formation of cytoplasmic DNA was quantitatively measured by a cell death detection ELISA kit. *Columns,* mean ($n = 3$); *bars,* SD.

transcriptionally repressed these Ku proteins in melanoma cells (28). However, none of these agents showed appreciable effect on suppressing the expression level of Ku70 or Ku80 (Fig. 2*A*).

To evaluate the drug effect on Ku70 acetylation, cell lysates of DU-145 cells treated with individual agents at the indicated concentrations for 24 h were immunoprecipitated with anti-Ku70 followed by immunoblotting with antibodies against acetyl-lysine, Ku80, and Ku70, respectively (Fig. 2*B*). As shown, these four inhibitors increased the acetylation level of Ku70 despite differences in their isozyme specificities. Moreover, acetylation of Ku70 did not affect its complex formation with Ku80 as the ratio of these two proteins in the immunoprecipitates remained unchanged.

HDAC inhibition diminishes cellular ability to repair DNA DSBs. Subsequently, the effect of acetylation on the DNA end-binding activity of Ku70 in nuclear extracts was examined after exposing DU-145 cells to different doses of OSU-HDAC42 and MS-275 for 24 h. As shown in Fig. 2*C*, these two HDAC inhibitors reduced the binding affinity of Ku70 to broken DNA ends with $IC_{50} < 0.25$ μmol/L and $IC_{50} < 0.5$ μmol/L, respectively.

In the literature, phosphorylation of histone H2AX (γH2AX) has been widely used as a biomarker for drug-induced DNA damage in light of its occurrence at sites flanking DNA DSBs (29). Pursuant to the above finding, we assessed the effect of OSU-HDAC42 on the level of γH2AX in DU-145 cells treated with bleomycin, doxorubicin, or VP-16. Figure 3*A* depicts the immunochemical analysis of γH2AX foci formation in DU-145 cells treated with 0.25 μmol/L OSU-HDAC42 in 10% FBS-supplemented medium for 4 h followed by bleomycin (10 μg/mL), doxorubicin (50, 100, and 200 nmol/L), or VP-16 (10 μmol/L) for 1 h. Although OSU-HDAC42 had no

appreciable effect on γH2AX phosphorylation levels, the sequential treatment significantly increased the number of γH2AX foci-positive cells compared with individual chemotherapeutic agents alone ($P < 0.05$; Fig. 3*A* and *B*). As shown in Fig. 3*A*, the extent of γH2AX formation increased with elevating concentrations of doxorubicin in OSU-HDAC42-pretreated DU-145 cells, indicating that OSU-HDAC42 could potentiate the dose-dependent effect doxorubicin on DNA damage. Moreover, the ability of OSU-HDAC42 to enhance the extent of drug-mediated γH2AX formation was shown by Western blotting and flow cytometry (Fig. 3*C* and *D*). Flow analysis indicates a 3- to 5-fold increase in DNA DSBs in response to OSU-HDAC42 pretreatment.

Pursuant to the above finding, we further examined the sensitizing effect of MS-275, a class I HDAC-specific inhibitor, on doxorubicin-induced DNA DSBs in DU-145 cells as well as that of OSU-HDAC42 in the Bax-intact PC-3 and LNCaP cells. As shown in Fig. 4*A*, despite a narrower spectrum of isozyme specificity than that of OSU-HDAC42, MS-275 was effective in augmenting the drug-induced γH2AX formation. This finding suggests that this chemosensitization was associated with the function of class I HDAC isozymes. Moreover, compared with DU-145 cells, PC-3 and LNCaP cells were equally susceptible to the sensitizing effect of OSU-HDAC42 despite differences in the status of Bax expression (Fig. 4*B*).

Constitutive acetylation of lysine residues in DNA-binding domains mimics HDAC inhibitors in suppressing the end-binding affinity of Ku70. Ku70 contains two DNA-binding domains. One is located at the NH_2 terminus before residue 440, and the other one resides in the COOH terminus (residues 536–609; refs. 5–8). These two domains differ in their dependence on Ku80 for the DNA-binding activity. Whereas the NH_2-terminal domain requires the participation of Ku80 to bind broken DNA ends, the DNA-binding activity of the COOH-terminal domain is independent of the heterodimer formation with Ku80. Moreover, the COOH-terminal DNA-binding domain encompasses the Bax-binding domain (9, 10, 12). It has been shown that mimicking a

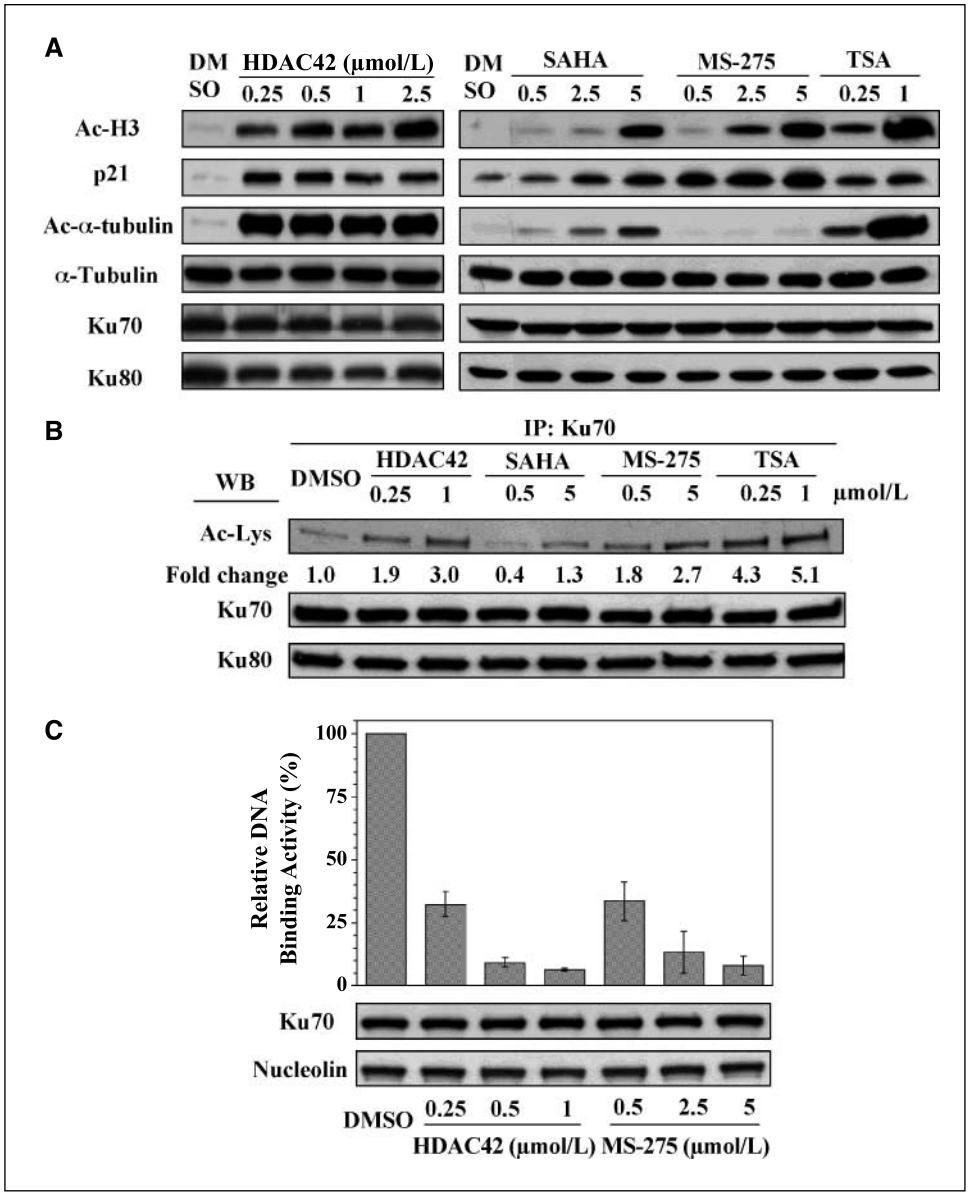

Figure 2. HDAC inhibitor-mediated Ku70 acetylation and its effect on the DNA end-binding activity of Ku70 in DU-145 cells. *A,* dose-dependent effect of four different HDAC inhibitors, including OSU-HDAC42, SAHA, MS-275, and TSA, on histone H3 acetylation (*Ac-H3*), p21 expression, α-tubulin acetylation, and Ku70 and Ku80 expression. Cells were treated with individual inhibitors at the indicated concentrations for 24 h, and the cell lysates were immunoblotted. *B,* dose-dependent effect of HDAC inhibitors on Ku70 acetylation. DU-145 cells were treated with individual inhibitors at the indicated concentrations for 24 h, and the cell lysates were immunoprecipitated with anti-Ku70 antibodies, and the immunoprecipitates were probed with anti-Ku70, anti-Ku80, and anti-pan-acetylated lysine (*Ac-Lys*) antibodies. The values denote the relative intensity of protein bands of drug-treated samples to that of the DMSO vehicle-treated control, after being normalized to the respective Ku70. Each value represents the average of two independent experiments. *C,* dose-dependent effect of OSU-HDAC42 and MS-275 on the DNA end-binding activity of Ku70 in nuclear extracts. Cells were treated with either agent at the indicated concentrations for 24 h, and Ku70 was extracted by the Nuclear Extract kit, and the DNA end-binding activity of Ku70 was quantitatively measured by a Ku70 DNA Repair kit. Equal amounts of Ku70 proteins were used for the assay as shown by immunoblotting against Ku70 and nucleolin. *Columns,* mean ($n = 3$); *bars,* SD.

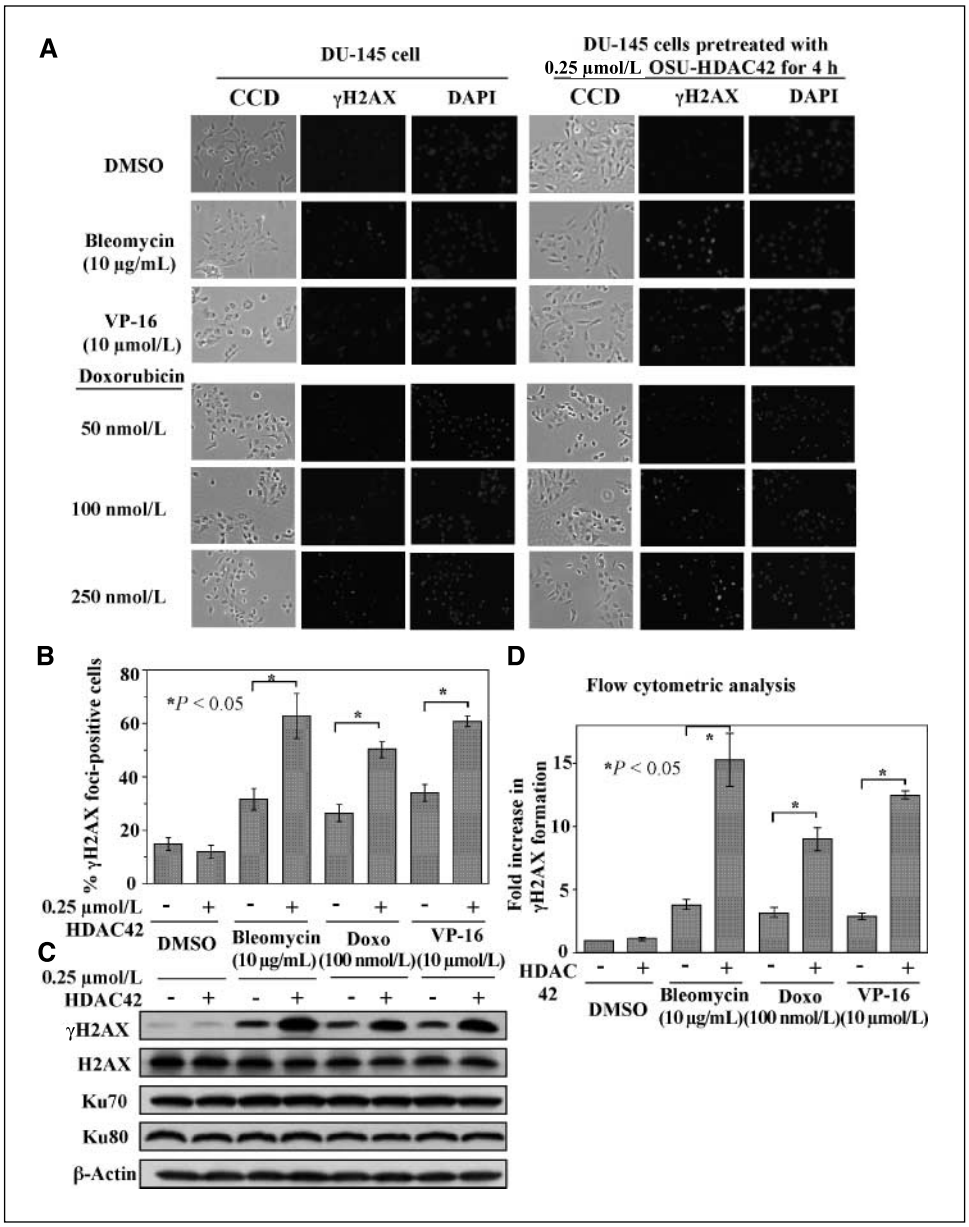

Figure 3. Effect of OSU-HDAC42 on enhancing drug-induced γH2AX foci formation in DU-145 cells. *A,* immunocytochemical analysis of the effect of OSU-HDAC42 on drug-induced γH2AX foci. Detection of γH2AX formation was carried out as described in Materials and Methods. Images were obtained by fluorescence microscopy. Representative γH2AX and DAPI-stained nuclei. *B,* percentage γH2AX foci-positive cells in drug-treated versus DMSO-treated DU-145 cells. Numbers of γH2AX foci-positive cells were counted in ~300 nuclei in each treatment group. Cells with more than five foci per nucleus were classified as γH2AX foci-positive cells. *Columns,* mean (n = 3); *bars,* SD. *, $P < 0.05$, Student's t test. *C,* Western blot analysis of the effect of OSU-HDAC42 on drug-induced H2AX phosphorylation and the expression levels of Ku70 and Ku80. *D,* flow cytometric analysis of the effect of OSU-HDAC42 on drug-induced H2AX phosphorylation. *Columns,* mean (n = 3); *bars,* SD. *, $P < 0.05$, Student's t test. *Doxo,* doxorubicin.

constitutively acetylated state of K539 or K542 by replacing it with glutamine (K → Q) abolished the Ku70-Bax interaction, thereby promoting Bax-mediated apoptosis (12).

As the Ku heterodimer interacts with DNA through electrostatic interactions between its positively charged residues and the sugar-phosphate backbone of DNA (22, 30), we hypothesized that acetylation of lysine residues would diminish the DNA-binding activity of Ku70. This mode of regulation was reminiscent to that of human Flap endonuclease-1 (31) and the transcription factor IFN regulatory factor-7 (32) reported in the literature.

To validate this hypothesis, we carried out site-directed mutagenesis to replace each of the following six lysine residues of Ku70 with glutamine, K282, K317, K331, K338, K539, and K542, to mimic constitutive acetylation. Of these six residues, K282, K317, K331, and K338 are located within the ring region, whereas K539 and K542 lie within the COOH-terminal linker of Ku70. These lysine residues, except K282, have been identified to be acetylated *in vivo* (12), and K282, K338, K539, and K542 have been implicated in DNA binding by X-ray structures (22, 30).

DU-145 cells were transfected with expression vectors encoding Flag-tagged wild-type (WT) or each of these Ku70 mutants via nucleofection. Western blotting indicates that these ectopic Ku70s were expressed at levels severalfold higher than that of the endogenous protein (Fig. 5*A*). Equal amounts of nuclear extracts (2.5 μg) of these transfected cells were analyzed for their ability to bind DNA broken ends. As shown in Fig. 5*B*, constitutive acetylation at K282, K338, K539, and K542 suppressed the DNA end-binding activity by 40% to 60% ($P < 0.005$), whereas substitution of K317 or K331 with glutamine had no significant effect. It is interesting to note that the dual mutation at K282 and K338 (K282Q/K338Q) or replacement of all four lysine residues at the NH_2-terminal DNA-binding domain (K282Q/K317Q/K331Q/K338Q) did not cause a higher degree of inhibition than that of K282Q or K338Q alone. This finding suggests that endogenous Ku70 contributed to the

residual activity in the nuclear extracts of these transfected cells. In contrast, the double mutant K317Q/K331Q had no significant effect on suppressing the DNA end-binding activity, confirming that neither lysine residue played a role in interacting with DNA.

Molecular modeling analysis. To envisage the spatial arrangement of these six lysine residues relative to the sugar-phosphate backbone of DNA, we carried out molecular modeling analysis by docking a 34-bp duplex into the DNA-binding channel of the Ku heterodimer (Ku70, Ku80, and broken DNA are colored in light blue, red, and yellow, respectively). Figure 5*C* depicts a consensus mode of Ku-DNA complex formation based on 50 docking simulations. Of the six residues examined, K282, K317, K331, and K338 are located within the region of Ku70 DNA-binding cradle, whereas the other two, K539 and K542, lie in COOH-terminal linker of Ku70. However, the mean distance between the ω-amino moiety of individual lysine residue and the phosphate backbone of DNA varied to different extent. The distance was ~3.5 Å for K282, K338, K539, and K542, in contrast to 17.4 and 4.6 Å for K317 and K331, respectively. As both K317 and K331 were pointed outward the DNA-binding ring, they were not within the effective range of electrostatic interactions with the DNA.

Constitutive acetylation of Ku70 diminishes the cellular ability to repair DNA DSBs. We also examined the effect of the constitutive acetylation at K282 and K338 on augmenting drug-induced γH2AX foci formation. DU-145 cells were transiently transfected with a pCMV plasmid (mock) or individual plasmids encoding Flag-tagged WT Ku70 and the mutants K282Q and K338Q. These cells were treated with 10 μg/mL bleomycin, 100 nmol/L doxorubicin, 10 μmol/L VP-16, or DMSO vehicle for 1 h, and the formation of γH2AX foci was assessed by immunocytochemistry (Fig. 6*A*). Immunostaining with anti-Flag antibodies indicates that ectopic Ku70 was expressed in nearly all cells examined. Compared with mock, overexpression of WT Ku70 did not suppress drug-induced γH2AX formation (Fig. 6*B*). One plausible explanation for this lack of protection was that the Ku70-overexpressing cells might not have stoichiometric quantities of Ku80 to form heterodimeric Ku complexes. In contrast, overexpression of K282Q or K338Q rendered cells more susceptible to doxorubicin-induced γH2AX foci formation and inhibition of clonogenic survival ($P < 0.05$; Fig. 6*B–D*).

Discussion

In this study, we report a unique histone acetylation-independent mechanism by which HDAC inhibitors sensitize prostate cancer cells to DNA-damaging agents through the regulation of the acetylation status of Ku70. It is well understood that Ku70 plays a dual role in repairing DNA DSBs and in suppressing Bax-mediated apoptosis by interacting with Ku80 and Bax, respectively, in different cellular compartments (12). These cytoprotective functions of Ku70 are abrogated in HDAC inhibitor-treated cells due to hyperacetylation, thereby rendering cancer cells more susceptible to the killing effect of DNA damage. This mechanistic finding has therapeutic relevance in terms of the combinatorial use of these

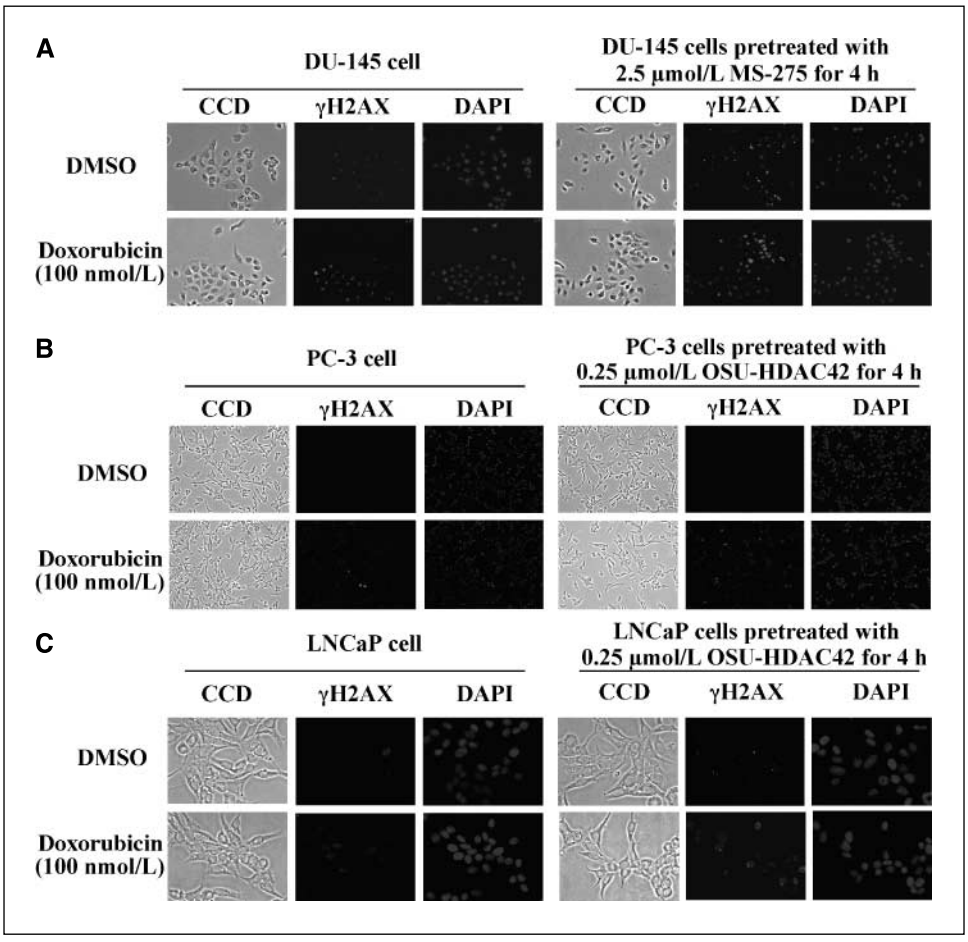

Figure 4. Immunocytochemical analysis of the effect of 2.5 μmol/L MS-275 on enhancing doxorubicin-induced γH2AX foci formation in DU-145 cells (*A*), the effect of 0.25 μmol/L OSU-HDC42 on enhancing doxorubicin-induced γH2AX foci formation in PC-3 cells (*B*), and the effect of 0.25 μmol/L OSU-HDC42 on enhancing doxorubicin-induced γH2AX foci formation in LNCaP cells (*C*). Detection of γH2AX formation was carried out as described in Materials and Methods. Images were obtained by fluorescence microscopy. Representative γH2AX and DAPI-stained nuclei.

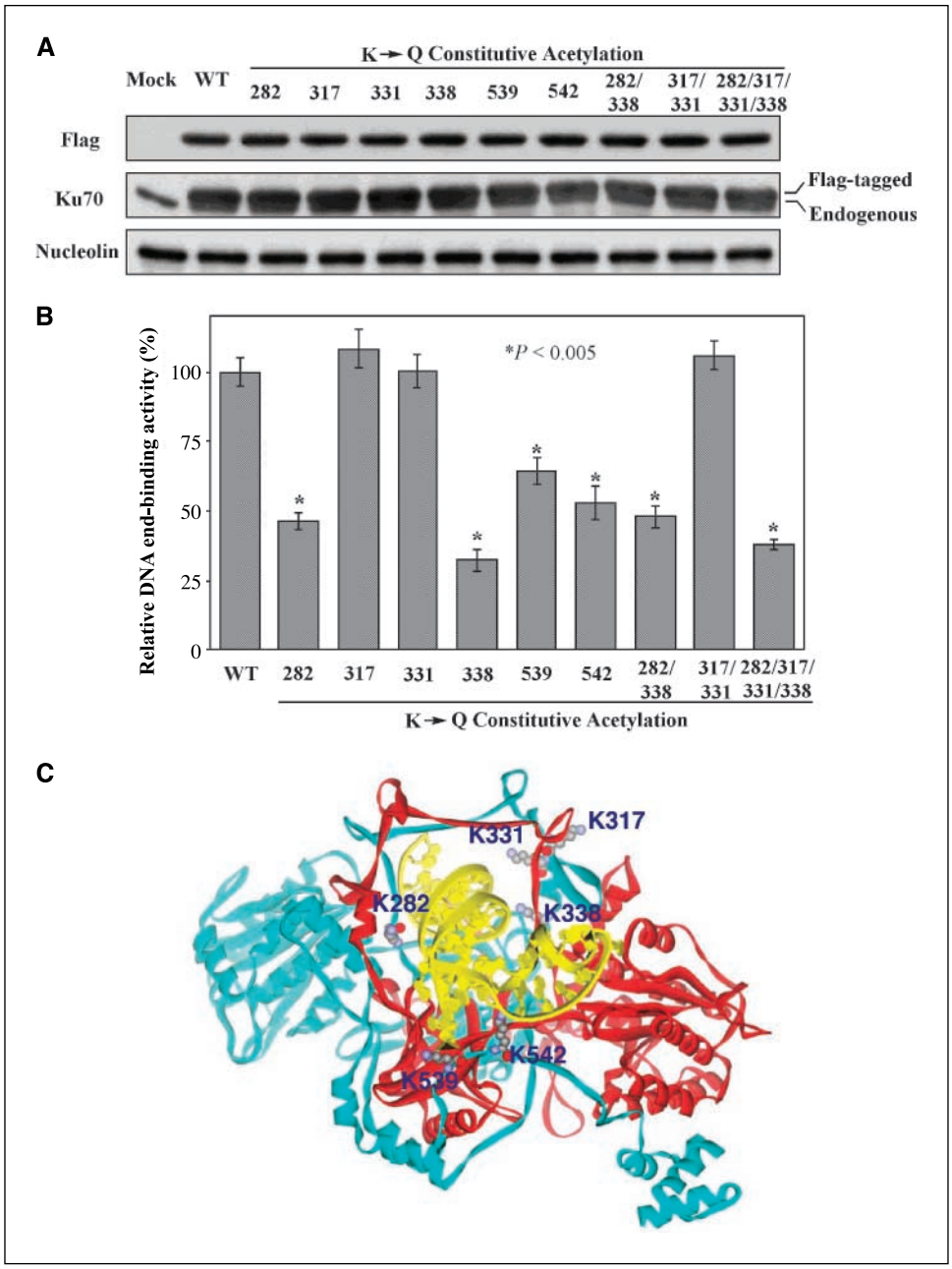

Figure 5. Effect of constitutive acetylation of lysine residues in the DNA-binding cradle of Ku70 on its DNA end-binding activity. DU-145 cells were nucleofected with a pCMV plasmid (mock) or individual plasmids encoding Flag-tagged WT Ku70 or the Ku70 mutants K282Q, K317Q, K331Q, K338Q, K539Q, and K542Q. After 48 h, Ku70 was extracted by using a Nuclear Extract kit. *A,* Western blot analysis of the expression level of Flag-tagged Ku70 versus endogenous Ku70 in nuclear extracts. *B,* relative DNA end-binding activity of individual Ku70 mutants to WT Ku70. The DNA end-binding activity of ectopic Ku70 was quantitatively measured by a Ku70 DNA Repair kit. *Columns,* mean ($n = 3$); *bars,* SD. *, $P < 0.05$ compared with cells transfected with WT Ku70 (WT) by Student's *t* test. *C,* molecular modeling analysis of the mode of interactions between the Ku heterodimer and DNA. Ku70 (*light blue*), Ku80 (*red*), and broken DNA (*yellow*). The six lysine residues that underwent site-mutagenesis are indicated.

two types of antitumor agents in cancer therapy. To achieve optimal therapeutic benefits, it might be desirable to use HDAC inhibitors preceding that of DNA-damaging agents.

Our data indicate that TSA, MS-275, SAHA, and OSU-HDAC42 caused Ku70 hyperacetylation despite differences in their HDAC isozyme specificities. Relative to other three agents, MS-275 exhibits a narrower spectrum of specificity with activity against HDAC1, HDAC2, and HDAC3, which is reflected in its inability to facilitate α-tubulin acetylation, a biomarker for inhibiting HDAC6. Nevertheless, MS-275 was equally efficacious in facilitating Ku70 acetylation as the broader spectrum inhibitors OSU-HDAC42 and TSA, suggesting that Ku70 acetylation might be associated with the function of HDAC1, HDAC2, and/or HDAC3.

In the literature, several different mechanisms have been proposed to account for the ability of HDAC inhibitors to radiosensitize or chemosensitize cancer cells. For example, sodium butyrate has been reported to reduce the gene expression of Ku70 and Ku80 in human melanoma cells (28) and to increase DNA topoisomerase IIα expression in human leukemic cells (33). Moreover, phenylbutyrate, but not sodium butyrate, was shown to potentiate the cytotoxic effect of doxorubicin in multidrug-resistant cancer cells by suppressing the activity of antioxidant enzymes, such as superoxide dismutase and glutathione reductase (34). Another school of thought is that histone acetylation conferred an open chromatin structure, thereby increasing the efficiency of anticancer agents targeting DNA (27). These multiple mechanisms underscore the pleiotropic effects of HDAC inhibitors at both epigenetic and cellular levels. However, in this study, we did not find the repression of Ku70 or Ku80 in OSU-HDAC42-treated DU-145 cells, which was in contrast to what was noted in sodium

butyrate–treated melanoma cells. The discrepancy might be attributable to differences in the transcriptional regulation of Ku proteins among different cell lines.

The DNA-binding cradle of Ku70 contains multiple lysine residues to form a positively charged lining for interacting with broken DNA ends (12, 22), many of which are acetylated *in vivo* (12). Our data indicate that Ku70 hyperacetylation would not disrupt the complex formation with Ku80. However, not all of these lysine residues were involved in interacting with DNA. Of the six lysine residues examined (K282, K317, K331, K338, K539, and K542), constitutive acetylation of K317 and K331 had no appreciable effect on reducing binding affinity with DNA broken ends. The bystander role of these two lysine residues was further confirmed by computer modeling data, indicating that they were not within an effective range to exert electrostatic interactions with the sugar-phosphate backbone of DNA. Previously, it was reported that substitution of either K539 or K542 in the COOH-terminal linker abolished the ability of Ku70 to bind Bax, thereby facilitating Bax-mediated apoptosis. Here, we report that these two lysine residues also took part in binding DNA broken ends. The dual binding partners of the COOH-terminal linker underline the crucial role of Ku70 in determining the fate of cells that have undergone DNA damage and provide a basis to design an effective strategy for the therapeutic combination of HDAC inhibitors with cytotoxic agents.

In conclusion, data from this and other laboratories have shown the *in vivo* efficacy of HDAC inhibitors, such as SAHA and OSU-HDAC42 as single-agent antitumor drugs, which target multiple aspects of cancer cell survival and cell cycle progression, including Akt signaling, mitochondrial integrity, and caspase activity. The ability of HDAC inhibitors to regulate cellular capacity to repair DNA damage through the modulation of the acetylation status of Ku70 underscores the viability of their use in tumor types that would benefit from sensitization to DNA-damaging therapeutic modalities. In prostate cancer, DNA-damaging cytotoxic agents are infrequently used clinically. Although such agents, like the topoisomerase II inhibitors doxorubicin and VP-16, are active in

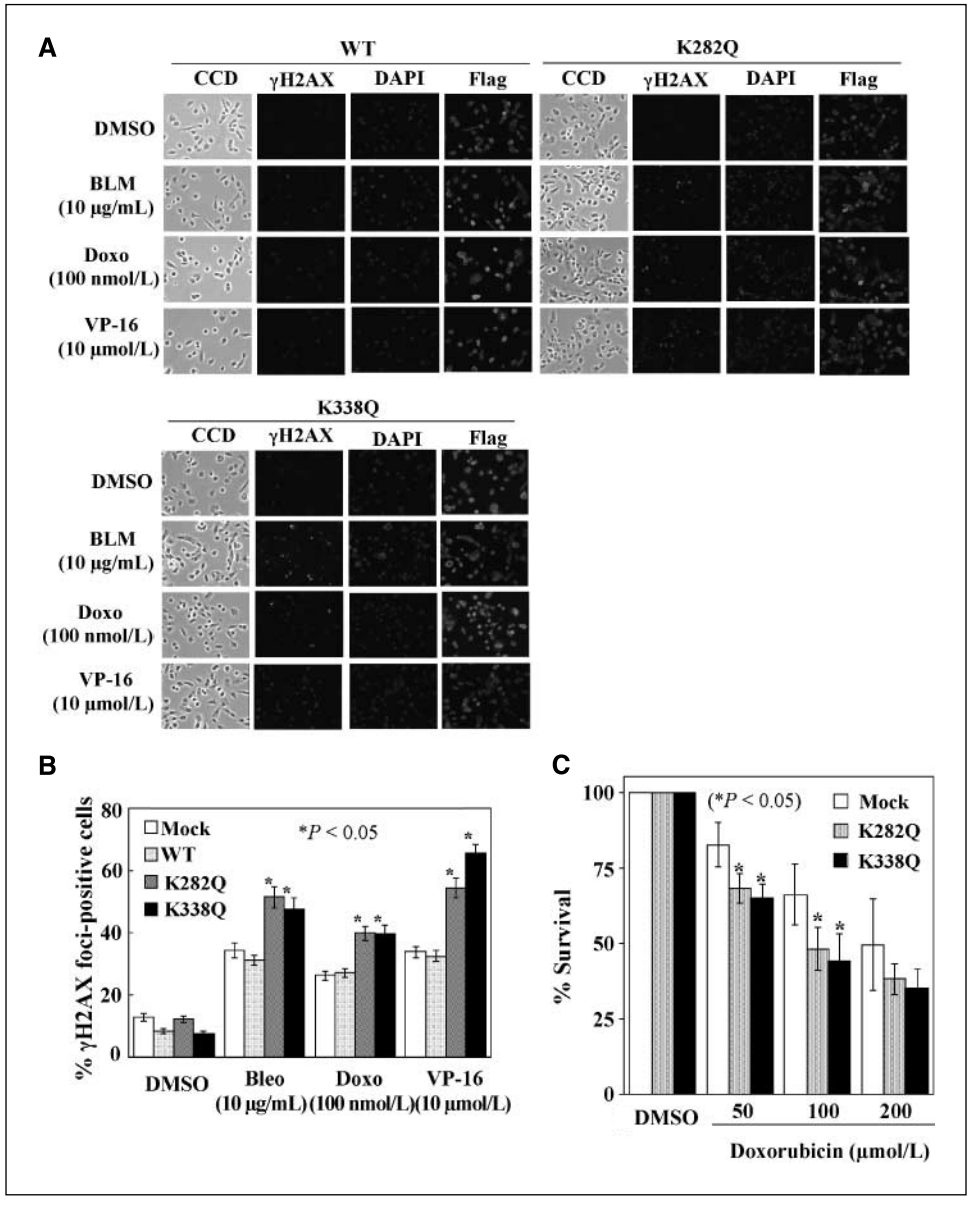

Figure 6. Effects of the constitutive acetylation of K282 and K338 of Ku70 on drug-induced γH2AX foci formation. *A,* immunocytochemical analysis of the constitutive acetylation on drug-induced γH2AX foci formation. DU-145 cells were nucleofected with individual plasmids encoding Flag-tagged WT, K282Q, and K338Q Ku70. After 48 h, cells were treated with bleomycin, doxorubicin, or VP-16 for 1 h and immunostained with antibodies against γH2AX and Flag. Images were obtained by fluorescence microscopy. *B,* percentage γH2AX foci-positive cells in response to drug treatment. *Columns,* mean ($n = 3$); *bars,* SD. *, $P < 0.005$, Student's *t* test. *C,* effect on clonogenic cell survival. *Columns,* mean ($n = 3$); *bars,* SD. *, $P < 0.005$, Student's *t* test. *Bleo,* bleomycin.

chemotherapeutic combinations against prostate cancer (35–39), their widespread clinical use has been limited by toxicities and lack of definitive survival benefits, particularly compared with recent advances showing improved survival with docetaxel-based strategies (40, 41). Nonetheless, these agents continue to be assessed in clinical trials for prostate cancer as components of chemotherapeutic combinations, in different formulations, and in the form of later generation analogues (39, 42). The results of the present study provide a rationale for the inclusion of modulators of Ku70 acetylation in clinical trials that involve these DNA-damaging agents for the treatment of prostate cancer patients. Although not directly evaluated in the present study, it is also likely that acetylation of Ku70 will sensitize cancer cells to the effects of ionizing radiation. As radiotherapy is a mainstay of prostate cancer treatment, the inclusion of HDAC inhibitors with this activity in preclinical studies and clinical trials of chemoradiotherapy for prostate cancer seem warranted. The results reported here characterize a unique mechanism of HDAC inhibitor-mediated perturbation of DNA damage repair in prostate cancer cells and provide a rationale for their inclusion in strategies to sensitize cancer cells to therapies that induce DNA damage.

Acknowledgments

Received 10/30/2006; revised 2/22/2007; accepted 3/20/2007.

Grant support: National Cancer Institute Public Health Service grant CA112250 and Department of Defense Prostate Cancer Research Program grant W81XWH-05-1-0089. William R. Hearst Foundation and Prostate Cancer Foundation awards.

The costs of publication of this article were defrayed in part by the payment of page charges. This article must therefore be hereby marked *advertisement* in accordance with 18 U.S.C. Section 1734 solely to indicate this fact.

References

1. Bolden JE, Peart MJ, Johnstone RW. Anticancer activities of histone deacetylase inhibitors. Nat Rev Drug Discov 2006;5:769–84.
2. Lin HY, Chen CS, Lin SP, Weng JR, Chen CS. Targeting histone deacetylase in cancer therapy. Med Res Rev 2006;26:397–413.
3. Chen CS, Weng SC, Tseng PH, Lin HP, Chen CS. Histone acetylation-independent effect of histone deacetylase inhibitors on Akt through the reshuffling of protein phosphatase 1 complexes. J Biol Chem 2005;280:38879–87.
4. Weterings E, van Gent DC. The mechanism of non-homologous end-joining: a synopsis of synapsis. DNA Repair (Amst) 2004;3:1425–35.
5. Chou CH, Wang J, Knuth MW, Reeves WH. Role of a major autoepitope in forming the DNA binding site of the p70 (Ku) antigen. J Exp Med 1992;175:1677–84.
6. Wang J, Dong X, Myung K, Hendrickson EA, Reeves WH. Identification of two domains of the p70 Ku protein mediating dimerization with p80 and DNA binding. J Biol Chem 1998;273:842–8.
7. Wang J, Dong X, Reeves WH. A model for Ku heterodimer assembly and interaction with DNA. Implications for the function of Ku antigen. J Biol Chem 1998;273:31068–74.
8. Wu X, Lieber MR. Protein-protein and protein-DNA interaction regions within the DNA end-binding protein Ku70–86. Mol Cell Biol 1996;16:5186–93.
9. Sawada M, Hayes P, Matsuyam S. Cytoprotective membrane-permeable peptides designed from the Bax-binding domain of Ku70. Nat Cell Biol 2003;5:352–7.
10. Sawada M, Sun W, Hayes P, Leskov K, Boothman DA, Matsuyama S. Ku70 suppresses the apoptotic translocation of Bax to mitochondria. Nat Cell Biol 2003;5:320–9.
11. Nothwehr SF, Martinou JC. A retention factor keeps death at bay. Nat Cell Biol 2003;5:281–3.
12. Cohen HY, Lavu S, Bitterman KJ, et al. Acetylation of the C terminus of Ku70 by CBP and PCAF controls Bax-mediated apoptosis. Mol Cell 2004;13:627–38.
13. Cohen HY, Miller C, Bitterman KJ, et al. Calorie restriction promotes mammalian cell survival by inducing the SIRT1 deacetylase. Science 2004;305:390–2.
14. Subramanian C, Opipari AW, Jr., Bian X, Castle VP, Kwok RP. Ku70 acetylation mediates neuroblastoma cell death induced by histone deacetylase inhibitors. Proc Natl Acad Sci U S A 2005;102:4842–7.
15. Lu Q, Wang DS, Chen CS, Hu YD, Chen CS. Structure-based optimization of phenylbutyrate-derived histone deacetylase inhibitors. J Med Chem 2005;48:5530–5.
16. Lu Q, Yang YT, Chen CS, et al. Zn^{2+}-chelating motif-tethered short-chain fatty acids as a novel class of histone deacetylase inhibitors. J Med Chem 2004;47:467–74.
17. Kulp SK, Chen CS, Wang DS, Chen CY, Chen CS. Antitumor effects of a novel phenylbutyrate-based histone deacetylase inhibitor, (S)-HDAC-42, in prostate cancer. Clin Cancer Res 2006;12:5199–206.
18. Kim JH, Shin JH, Kim IH. Susceptibility and radiosensitization of human glioblastoma cells to trichostatin A, a histone deacetylase inhibitor. Int J Radiat Oncol Biol Phys 2004;59:1174–80.
19. Fiser A, Do RK, Sali A. Modeling of loops in protein structures. Protein Sci 2000;9:1753–73.
20. Singh UC, Kollman PA. An approach to computing electrostatic charges for molecules. J Comp Chem 1984;5:129–45.
21. Morris GM, Goodsell DS, Halliday RS, et al. Automated docking using a Lamarckian genetic algorithm and an empirical free energy function. J Comp Chem 1998;19:1639–62.
22. Walker JR, Corpina RA, Goldberg J. Structure of the Ku heterodimer bound to DNA and its implications for double-strand break repair. Nature 2001;412:607–14.
23. Isaacs WB, Carter BS, Ewing CM. Wild-type p53 suppresses growth of human prostate cancer cells containing mutant p53 alleles. Cancer Res 1991;51:4716–20.
24. Yin MB, Rustum YM. Comparative DNA strand breakage induced by FUra and FdUrd in human ileocecal adenocarcinoma (HCT-8) cells: relevance to cell growth inhibition. Cancer Commun 1991;3:45–51.
25. Sampath D, Rao VA, Plunkett W. Mechanisms of apoptosis induction by nucleoside analogs. Oncogene 2003;22:9063–74.
26. Rochester MA, Riedemann J, Hellawell GO, Brewster SF, Macaulay VM. Silencing of the IGF1R gene enhances sensitivity to DNA-damaging agents in both PTEN wild-type and mutant human prostate cancer. Cancer Gene Ther 2005;12:90–100.
27. Kim MS, Blake M, Baek JH, Kohlhagen G, Pommier Y, Carrier F. Inhibition of histone deacetylase increases cytotoxicity to anticancer drugs targeting DNA. Cancer Res 2003;63:7291–300.
28. Munshi A, Kurland JF, Nishikawa T, et al. Histone deacetylase inhibitors radiosensitize human melanoma cells by suppressing DNA repair activity. Clin Cancer Res 2005;11:4912–22.
29. Banath JP, Olive PL. Expression of phosphorylated histone H2AX as a surrogate of cell killing by drugs that create DNA double-strand breaks. Cancer Res 2003;63:4347–50.
30. Zhang Y, Adachi M, Zou H, Hareyama M, Imai K, Shinomura Y. Histone deacetylase inhibitors enhance phosphorylation of histone H2AX after ionizing radiation. Int J Radiat Oncol Biol Phys 2006;65:859–66.
31. Hasan S, Stucki M, Hassa PO, et al. Regulation of human flap endonuclease-1 activity by acetylation through the transcriptional coactivator p300. Mol Cell 2001;7:1221–31.
32. Caillaud A, Prakash A, Smith E, et al. Acetylation of interferon regulatory factor-7 by p300/CREB-binding protein (CBP)-associated factor (PCAF) impairs its DNA binding. J Biol Chem 2002;277:49417–21.
33. Kurz EU, Wilson SE, Leader KB, et al. The histone deacetylase inhibitor sodium butyrate induces DNA topoisomerase IIα expression and confers hypersensitivity to etoposide in human leukemic cell lines. Mol Cancer Ther 2001;1:121–31.
34. Shack S, Miller A, Liu L, Prasanna P, Thibault A, Samid D. Vulnerability of multidrug-resistant tumor cells to the aromatic fatty acids phenylacetate and phenylbutyrate. Clin Cancer Res 1996;2:865–72.
35. Pienta KJ, Redman B, Hussain M, et al. Phase II evaluation of oral estramustine and oral etoposide in hormone-refractory adenocarcinoma of the prostate. J Clin Oncol 1994;12:2005–12.
36. Small EJ, Srinivas S, Egan B, McMillan A, Rearden TP. Doxorubicin and dose-escalated cyclophosphamide with granulocyte colony-stimulating factor for the treatment of hormone-resistant prostate cancer. J Clin Oncol 1996;14:1617–25.
37. Haas NB, Manola J, Hudes G, Citrin DL, Kies MS, Davis TE. Phase II pilot study of combined chemo-hormonal therapy with doxorubicin and estramustine in metastatic prostate cancer. Am J Clin Oncol 2000;23:589–92.
38. Smith DC, Chay CH, Dunn RL, et al. Phase II trial of paclitaxel, estramustine, etoposide, and carboplatin in the treatment of patients with hormone-refractory prostate carcinoma. Cancer 2003;98:269–76.
39. Borden LS, Jr., Clark PE, Lovato J, et al. Vinorelbine, doxorubicin, and prednisone in androgen-independent prostate cancer. Cancer 2006;107:1093–100.
40. Petrylak DP, Tangen CM, Hussain MH, et al. Docetaxel and estramustine compared with mitoxantrone and prednisone for advanced refractory prostate cancer. N Engl J Med 2004;351:1513–20.
41. Tannock IF, de Wit R, Berry WR, et al. Docetaxel plus prednisone or mitoxantrone plus prednisone for advanced prostate cancer. N Engl J Med 2004;351:1502–12.
42. Fiedler W, Tchen N, Bloch J, et al. A study from the EORTC new drug development group: open label phase II study of sabarubicin (MEN-10755) in patients with progressive hormone refractory prostate cancer. Eur J Cancer 2006;42:200–4.